

## Electronic Supplementary Information

### Nano-Engineering Safer-By-Design Nanoparticle Based Moth-Eye Mimetic Bactericidal and Cytocompatible Polymer Surfaces

Felipe Viela, Iván Navarro-Baena, Alejandra Jacobo, Jaime J. Hernández, Marta Boyano-Escalera, Manuel R. Osorio, Isabel Rodríguez\*

Madrid Institute for Advanced Studies in Nanoscience (IMDEA Nanoscience), C/Faraday 9, Ciudad Universitaria de Cantoblanco, Madrid 28049, Spain

\*Correspondence to: [i.rodriguez@imdea.org](mailto:i.rodriguez@imdea.org)

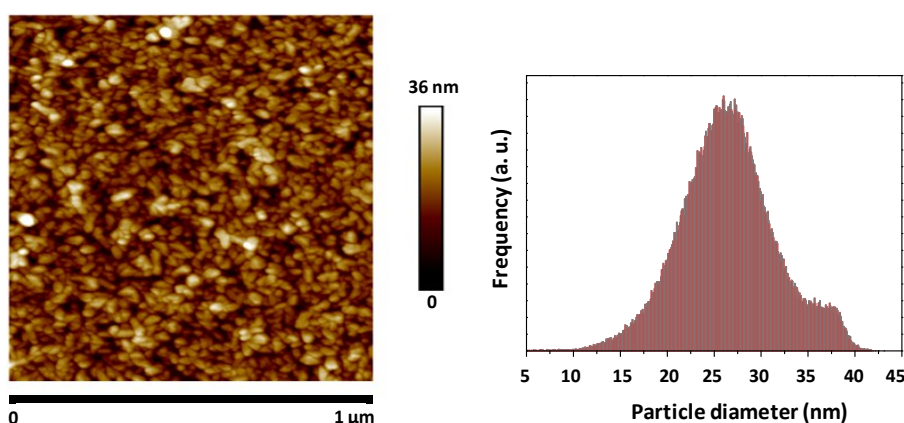


**Figure S1.** TiO<sub>2</sub> synthesized nanoparticle characterization: AFM image of TiO<sub>2</sub> layered nanoparticles prior imprinting obtained after spin coating a 0.5 wt% TiO<sub>2</sub> dispersion and extracted nanoparticle size distribution from the image (mean nanoparticle size: 26 nm).

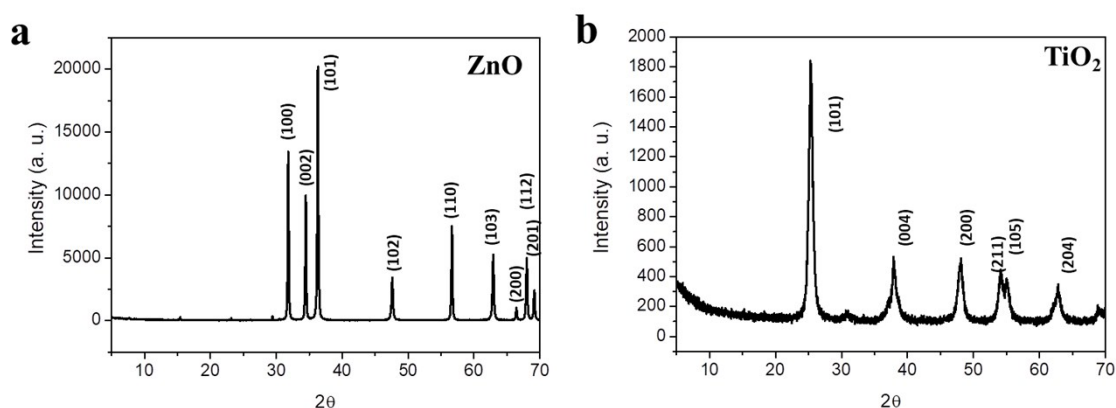


**Figure S2.** X-ray diffraction patterns of synthesized TiO<sub>2</sub> and ZnO nanoparticles. The observed diffraction peaks match well with the ZnO wurtzite crystal lattice parameters and with anatase TiO<sub>2</sub> crystal phase structure.

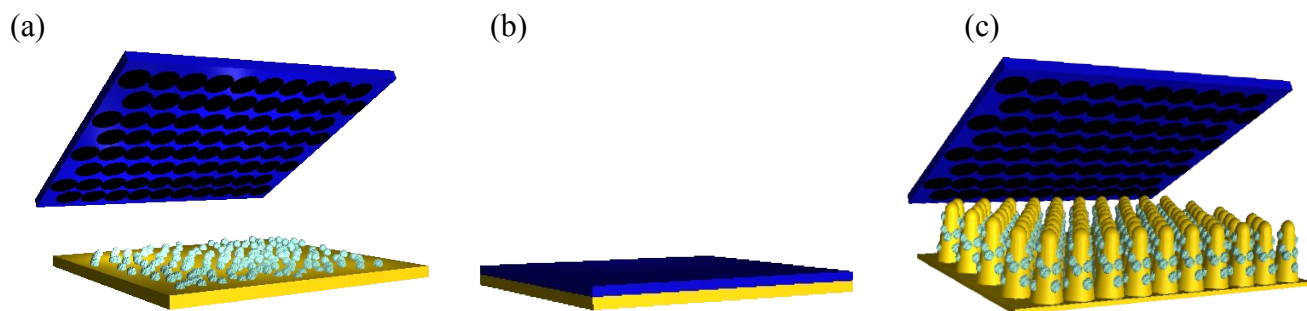


**Figure. S3.** Schematic illustration of the fabrication process of moth-eye nanocomposite surfaces involving the processes of a) nanoparticle coating, b) thermal nanoimprinting and c) de-molding

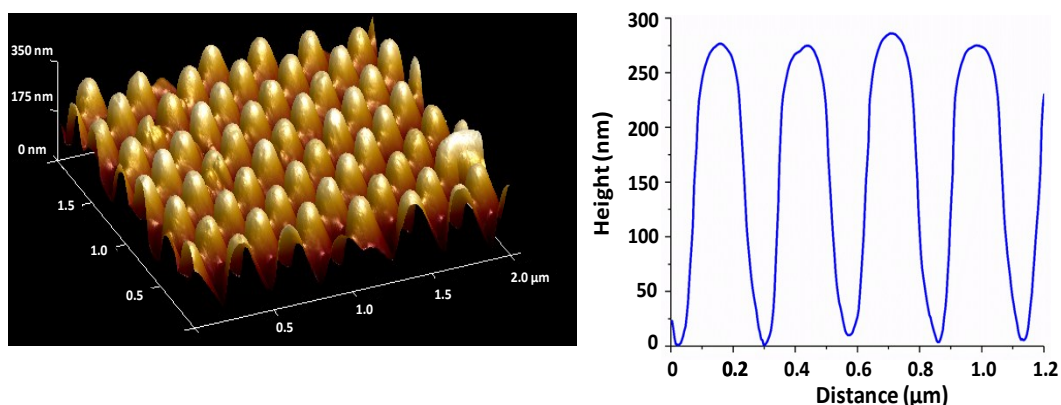


**Figure S4.** 3D AFM image and cross sectional profile of the imprinted moth-eye mimetic ZnO nanocomposite surfaces.

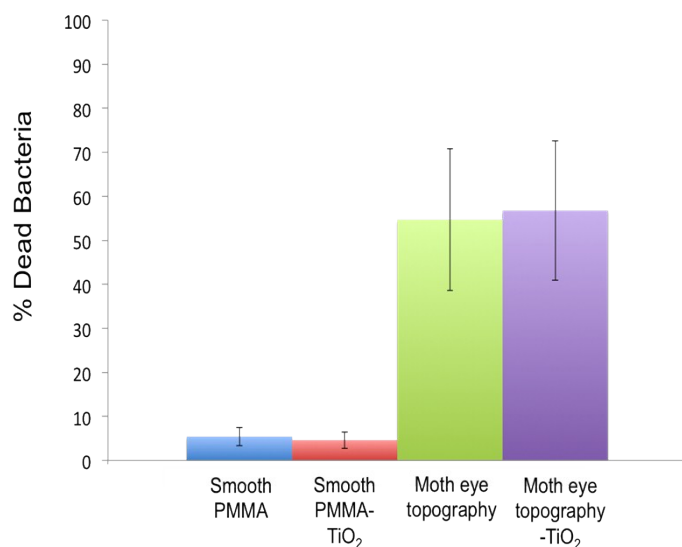


**Figure S5.** Comparative percentage of dead *S. aureus* cultured on smooth PMMA, smooth PMMA-TiO<sub>2</sub>, moth eye topography on neat PMMA and moth eye topography on PMMA-TiO<sub>2</sub> nanocomposite without UV light exposure. The number of dead bacteria on smooth and nanopatterned titania nanocomposites is comparable to the number of dead bacteria on

smooth and nanopatterned neat PMMA controls, indicating that there is not bactericidal action by the TiO<sub>2</sub> without light activation. The bactericidal action observed in this case corresponds to that effected by the topography.

1. Nanocomposite	Zn <sup>2+</sup> (µg/l)	Ti <sup>4+</sup> (µg/l)	2. Nanocomposite	Zn <sup>2+</sup> (µg/l)	Ti <sup>4+</sup> (µg/l)
<i>Control(H<sub>2</sub>O)*</i>	10.09	0.00	Control(Bacteria culture medium)	2.31	0.00
Moth eye ZnO nanocomposite	593.62	0.00	Moth eye ZnO nanocomposite	41.64	0.00
Moth eye TiO <sub>2</sub> nanocomposite	10.09	12.38	Moth eye TiO <sub>2</sub> nanocomposite	2.82	0.00

**Table S6.** Ion release from ZnO and TiO<sub>2</sub> nanocomposites

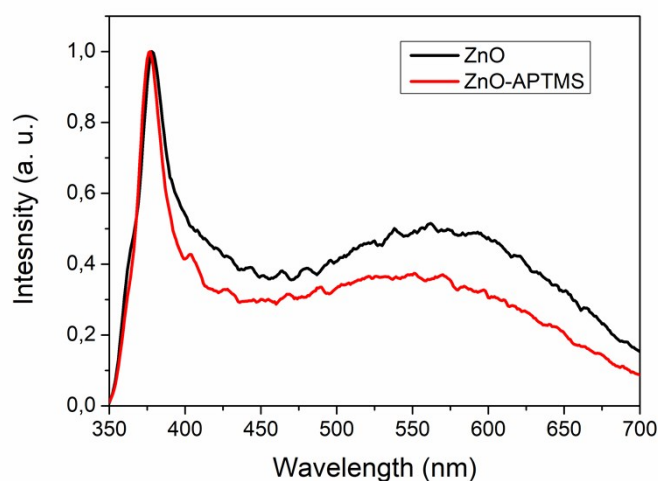


**Figure S7** Spectrum of photoluminescence of the ZnO nanoparticles in methanol under 325 nm excitation wavelength at room temperature obtained using a fluorospectrometer (FluoroLog 3, HORIBA). The PL spectrum shows a broad visible luminescence band from 400 to 700 nm originated from the defect states from zinc or oxygen vacancies.<sup>1</sup> The decrease in PL intensity in the visible region upon silanization indicates that the attached silane molecules on the surface of the ZnO nanoparticles produce a passivation of the surface defects.

<sup>1</sup> Raji, R., & Gopchandran, K. G. (2017). ZnO nanostructures with tunable visible luminescence: Effects of kinetics of chemical reduction and annealing. *Journal of Science: Advanced Materials and Devices*, 2(1), 51-58.

*Hydroxyl radical detection* by the reaction between terephthalic acid and hydroxyl radical with the formation of the fluorescent 2-hydroxyterephthalic acid.

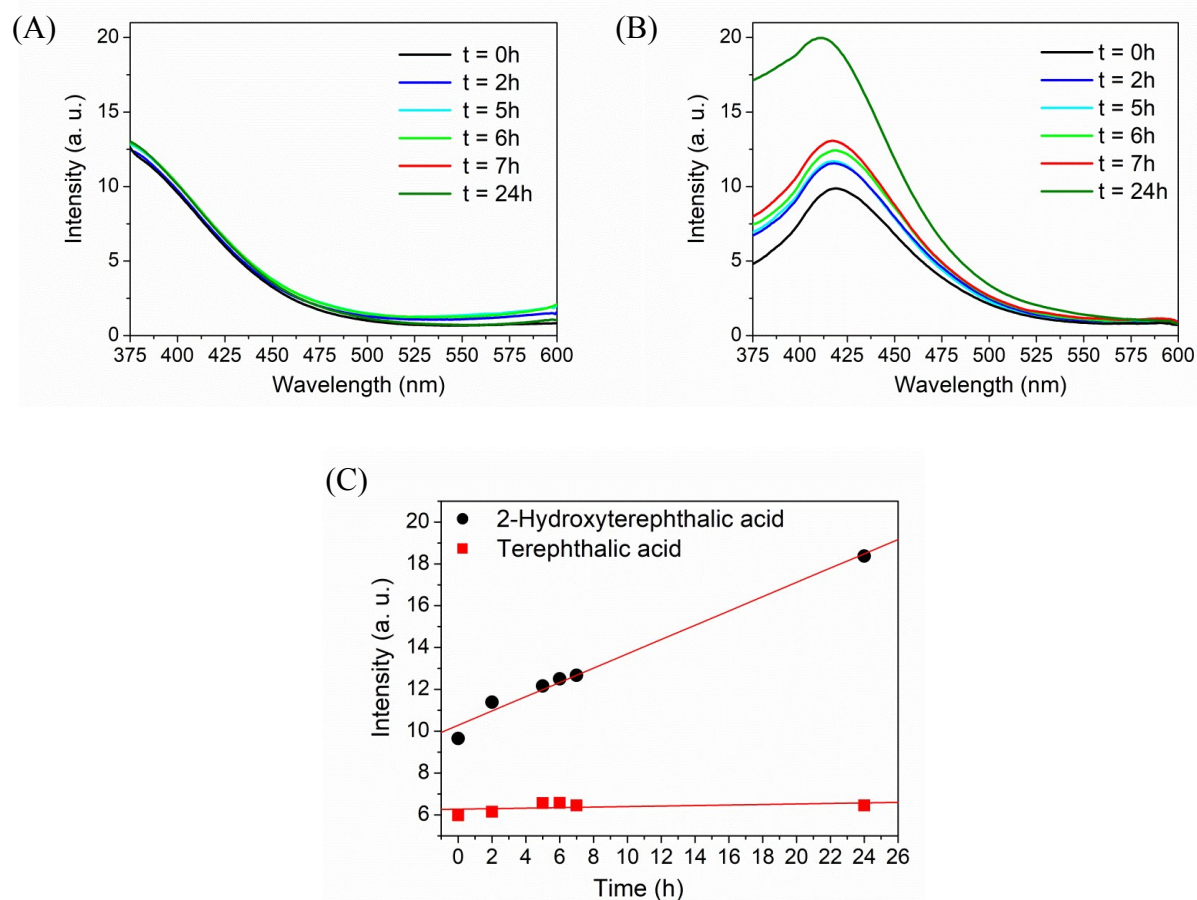


**Figure S8.** (A) Fluorescence spectrum of hydroxyl terephthalic acid in PB buffer in contact with moth eye ZnO nanocomposite surfaces. The terephthalic acid emission at different times was used as a control. (B) Variation of the 2-hydroxyterephthalic acid fluorescence emission at 425 nm with incubation time on the ZnO nanocomposite surfaces. (C) 2-hydroxyterephthalic acid formation kinetics

*Hydrogen peroxide detection* through reaction with Ampliflu red. The assay relies on the reaction of  $\text{H}_2\text{O}_2$  with the colorless Ampliflu Red to form the fluorescent resorufin in a reaction with a 1:1 stoichiometry catalyzed by horseradish peroxidase (HRP)

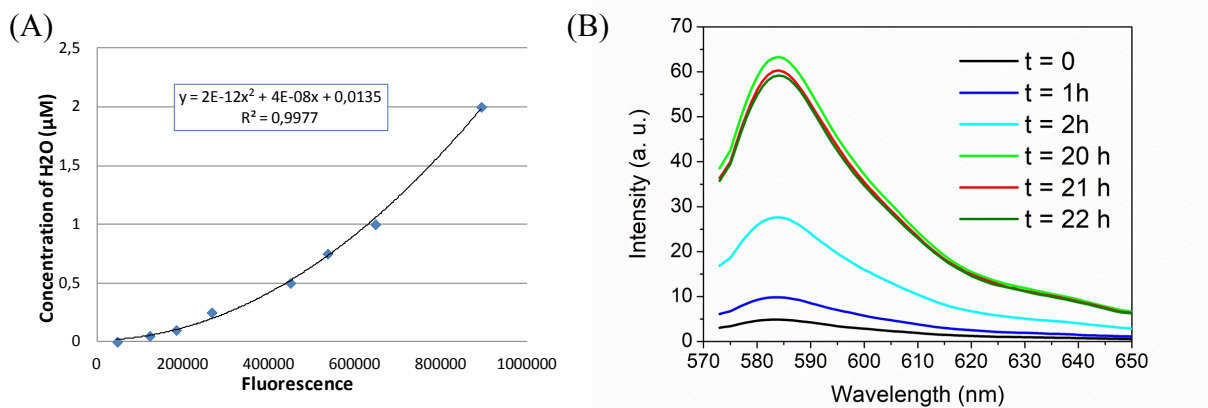


**Figure S9.** Ampliflu Red assay. (a)  $\text{H}_2\text{O}_2$  calibration curve. (b) Determination of the  $\text{H}_2\text{O}_2$  production by the ZnO nanocomposite surfaces in the dark over and an increasing period of time.